Smart Structures and Systems, *Vol. 24, No. 1 (2019) 83-94*
DOI: https://doi.org/10.12989/sss.2019.24.1.083

Impact of cable sag on the efficiency of an inertial mass damper in controlling stay cable vibrations

Zhi-hao Wang*[1], Hui Gao[1], Yan-wei Xu[1], Zheng-qing Chen[2] and Hao Wang[3]

[1]International Joint Research Lab for Eco-building Materials and Engineering of Henan Province, North China University of Water Resources and Electric Power, Zhengzhou 450045, China
[2] Key Laboratory for Wind and Bridge Engineering of Hunan Province, Hunan University, Changsha 410082, China
[3]Key Laboratory of Concrete and Pre-stressed Concrete Structure of Ministry of Education, Southeast University, Nanjing 210096, China

(Received October 11, 2018, Revised March 8, 2019, Accepted March 10, 2019)

Abstract. Passive negative stiffness dampers (NSDs) that possess superior energy dissipation abilities, have been proved to be more efficient than commonly adopted passive viscous dampers in controlling stay cable vibrations. Recently, inertial mass dampers (IMDs) have attracted extensive attentions since their properties are similar to NSDs. It has been theoretically predicted that superior supplemental damping can be generated for a taut cable with an IMD. This paper aims to theoretically investigate the impact of the cable sag on the efficiency of an IMD in controlling stay cable vibrations, and experimentally validate superior vibration mitigation performance of the IMD. Both the numerical and asymptotic solutions were obtained for an inclined sag cable with an IMD installed close to the cable end. Based on the asymptotic solution, the cable attainable maximum modal damping ratio and the corresponding optimal damping coefficient of the IMD were derived for a given inertial mass. An electromagnetic IMD (EIMD) with adjustable inertial mass was developed to investigate the effects of inertial mass and cable sag on the vibration mitigation performance of two model cables with different sags through series of first modal free vibration tests. The results show that the sag generally reduces the attainable first modal damping ratio of the cable with a passive viscous damper, while tends to increase the cable maximum attainable modal damping ratio provided by the IMD. The cable sag also decreases the optimum damping coefficient of the IMD when the inertial mass is less than its optimal value. The theoretically predicted first modal damping ratio of the cable with an IMD, taking into account the sag generally, agrees well with that identified from experimental results, while it will be significantly overestimated with a taut-cable model, especially for the cable with large sag.

Keywords: inertial mass damper; stay cable; vibration control; cable sag; modal damping ratio

1. Introduction

As key structural elements in long-span cable-stayed bridges, stay cables are prone to excessive vibrations due to their high flexibility and low inherent damping characteristics. Large oscillations may reduce lifespan of cables and have detrimental effects on public confidence in the safety of the bridge. Various countermeasures and control strategies have been proposed to mitigate cable vibrations (Pacheco *et al.* 1993, Chen *et al.* 2004, Wang *et al.* 2005, Christenson *et al.* 2006, Duan *et al.* 2006, Cai *et al.* 2007, Li *et al.* 2007, Jung *et al.* 2008, Kim *et al.* 2010, Huang *et al.* 2012, Shen *et al.* 2016, He *et al.* 2018). Among these methods, transversely attached passive viscous dampers have been widely implemented in real applications. However, only minimal supplemental damping can be provided to the cable since the damper is typically restricted to the vicinity of the bridge deck for aesthetic and practical reasons (Pacheco *et al.* 1993, Krenk 2000, Fujino and Hoang 2008, Zhou *et al.* 2014a). In addition, both the damper stiffness and the damper support stiffness have adverse effects on the damper control performance (Xu and Zhou 2007, Zhou and Sun 2008, Fournier and Cheng 2014, Zhou *et al.* 2014b). For long stay cables, such as Russky Island Bridge with 580 meters long cables, the supplemental damping induced by a passive viscous damper may be insufficient to suppress the problematic vibration of the cable (Weber and Distl 2015a). To solve this problem, combining cross-ties and dampers has been proposed, which was proved both theoretically and practically to be an effective method for long cables (Zhou *et al.* 2015, Ahmad *et al.* 2018).

Recently studies have demonstrated that the supplemental damping of stay cables with negative stiffness dampers (NSDs) are larger than those with passive viscous dampers (Li *et al.* 2008, Chen *et al.* 2015, Weber and Distl 2015b, Zhou and Li 2016, Shi *et al.* 2016, Wang *et al.* 2018). Li *et al.* (2008), Chen *et al.* (2015) and Shi *et al.* (2016) theoretically examined the dynamic behavior of a taut cable with a NSD. They showed that NSDs can provide considerable damping for stay cables, and the better control performance of NSDs is mainly attributed to the negative stiffness characteristic of the damper, which can increase

∗Corresponding author, Associate Professor
E-mail: wangzhihao@ncwu.edu.cn

http://www.techno-press.com/journals/sss&subpage=7
ISSN: 1738-1584 (Print), 1738-1991 (Online)

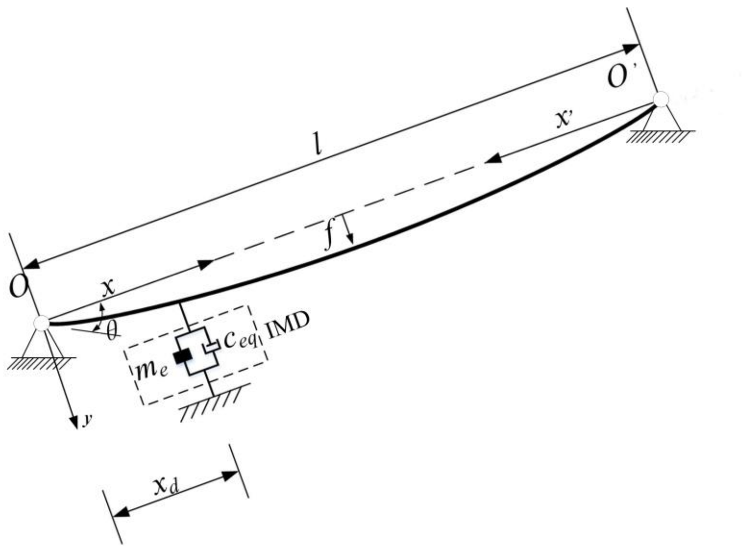

Fig. 1 Analysis model of an inclined sag cable with an IMD

the damper motion and enhance its energy dissipation ability. Zhou and Li (2016) experimentally demonstrated that a passive pre-spring NSD can provide superior first and second modal damping ratios of a cable subjected to both single-mode and multi-mode excitations. Shi *et al.* (2017) also verified that a passive magnetic NSD can offer an optimal modal damping ratio that is four times as large as that produced by a passive viscous damper.

Researchers have also proposed other means to achieve an effect that are similar to the NSD in a cable-damper system. Recent investigations showed that concentrated mass can demonstrate similar damping improvement effects as negative stiffness (Zhou *et al.* 2018b, Zhou *et al.* 2018c) However, to make significant increase to the attainable damping of the cable, a large mass is needed, which may be beyond the practical limits of the application (Lu *et al.* 2017). An alternative is to use a vibration suppression device incorporating an inerter. Inertial mass dampers (IMDs) have attracted extensive attentions since their inerters can generate an apparent mass that is two orders of magnitude higher than their physical mass (Ikago *et al.* 2012, Nakamura *et al.* 2014, Lazar *et al.* 2016, Lu *et al.* 2017, Sun *et al.* 2017, Shi and Zhu 2018, Zhu *et al.* 2019). Furthermore, the superior mitigation performance of typical IMDs, such as the viscous inertial mass damper (Lu *et al.* 2017, Shi and Zhu 2018, Cu *et al.* 2018) and the tuned inerter damper (Lazar *et al.* 2016, Sun *et al.* 2017, Luo *et al.* 2019), have been theoretically investigated and illustrated through an ideal taut-cable model that neglects the effects of cable sag. However, previous studies (Xu and Yu 1998, Krenk and Nielsen 2002, Johnson *et al.* 2003, Duan 2004, Christenson *et al.* 2006, Wang *et al.* 2018) have shown that cable sag has adverse effects on the efficiency of transverse dampers, especially for the first mode of the cable. For example, Xu and Yu (1998) illustrated that the first modal damping ratio of a 442.6m-long stay cable with a passive viscous damper was reduced by about 38%, compared to that predicted by a taut-cable model.

This paper aims to theoretically and experimentally evaluate the effect of the cable sag on the efficiency of an IMD in controlling cable vibrations. Both the numerical and asymptotic solutions were obtained for an inclined sag cable with an IMD installed close to the cable end. Based on the asymptotic solution, the cable attainable maximum modal damping ratio and the corresponding optimal damping coefficient of the IMD were derived for a given inertial mass. Subsequently, two model cables with different dynamic characteristics and sag parameters were established to experimentally verify the effect of cable sag on the mitigation performance of an IMD and to validate superior vibration mitigation performance of the IMD. Finally, the feasibility and applicability of the theoretical prediction results were evaluated by comparing the theoretical and the experimental supplemental first modal damping ratios of two model cables with sag.

2. Theoretical analysis of an inclined sag cable with an IMD

2.1 Model formulation

Fig. 1 shows an inclined sag cable with an IMD installed at the location $x = x_{\mathrm{d}}$. The IMD is represented by an inerter paralleled with a dashpot. Therefore, the IMD force F_{IMD} can be expressed as

$$F_{\mathrm{IMD}} = m_{\mathrm{e}}\ddot{y}(x_{\mathrm{d}},t) + c_{\mathrm{eq}}\dot{y}(x_{\mathrm{d}},t) \tag{1}$$

where m_{e} and c_{eq} denote the inertial mass and the equivalent damping coefficient, respectively; $\dot{y}(x_{\mathrm{d}},t)$ and $\ddot{y}(x_{\mathrm{d}},t)$ are the transient velocity and acceleration of the cable at the damper location, respectively.

By introducing the assumptions that: (1) the sag-to-span ratio is sufficiently small with respect to unity; (2) the cable vibrates only in the *x*-*y* plane and its motion in the *x*-direction is negligible; (3) the static profile of the cable $y_0(x, t)$ is a second-order parabola; (4) the flexural rigidity of the cable is ignored, the transverse free vibration of the cable-IMD system can be expressed as (Duan 2004)

$$-\frac{\partial^2}{\partial x^2}y(x,t)-\frac{\lambda^2}{l^3}\int_0^l y(x,t)\mathrm{d}x+\frac{m}{T_0}\frac{\partial^2 y(x,t)}{\partial t^2}+\frac{F_{\mathrm{IMD}}}{T_0}\delta(x-x_{\mathrm{d}})=0 \tag{2}$$

where

$y(x, t)$ is the cable vibration around its static profile $y_0(x,\ t)$,

T_0 is the tension force along the chord OO',

m is the mass per unit length,

l is the length of the cable,

$\delta(\cdot)$ is the Dirac delta function,

λ^2 is the sag-extensibility parameter (Irvine and Caughy 1974)

$$\lambda^2=\left(\frac{mgl\cos\theta}{T_0}\right)^2\frac{EAl}{T_0 L_e} \tag{3}$$

where g is the gravity acceleration, θ is the inclination angle, EA is the extensional rigidity of the cable and L_{e} is the static (stretched) length of the cable

$$L_{\mathrm{e}}\approx\left[1+\frac{1}{8}\left(\frac{mgl\cos\theta}{T_0}\right)^2\right]l \tag{4}$$

The concentrated force F_{IMD} triggers a discontinuity in $\partial y/\partial x$ at the IMD location $x=x_{\mathrm{d}}$, that is

$$T_0\frac{\mathrm{d}y(x_{\mathrm{d}}^{+})}{\mathrm{d}x}-T_0\frac{\mathrm{d}y(x_{\mathrm{d}}^{-})}{\mathrm{d}x}=F_{\mathrm{IMD}} \tag{5}$$

When the cable oscillates with the complex natural frequency ω, the cable vibration, the additional cable tension force, and the IMD force can be expressed as

$$y(x,t)=\tilde{y}(x)\exp(i\omega t),\ T=\tilde{T}(x)\exp(i\omega t),\ F_{\mathrm{IMD}}=\tilde{F}_{\mathrm{IMD}}\exp(i\omega t) \tag{6}$$

where $\tilde{y}(x)$, $\tilde{T}(x)$ and $\tilde{F}_{\mathrm{TID}}(x)$ denote the amplitude of cable displacement, the amplitude of additional cable tension force, and the amplitude of IMD force, respectively.

Considering the transverse displacement compatibility condition and the equilibrium condition at the IMD location, the wave number β of cable can be expressed as (Zhou *et al.* 2018a)

$$\begin{aligned}&\sin\left(\frac{\beta l}{2}\right)\left\{\sin\left(\frac{\beta l}{2}\right)-\cos\left(\frac{\beta l}{2}\right)\left[\frac{\beta l}{2}-\frac{4}{\lambda^2}\left(\frac{\beta l}{2}\right)^3\right]\right\}\\&=-2\left[\frac{1}{T_0\beta}\frac{\tilde{F}_{\mathrm{IMD}}}{\tilde{y}_{\mathrm{d}}}\right]\sin\left(\frac{\beta x_{\mathrm{d}}}{2}\right)\sin\left(\frac{\beta x_{\mathrm{d}}'}{2}\right)\left\{\sin\left(\frac{\beta l}{2}\right)-\cos\left(\frac{\beta x_{\mathrm{d}}}{2}\right)\cos\left(\frac{\beta x_{\mathrm{d}}'}{2}\right)\left[\frac{\beta l}{2}-\frac{4}{\lambda^2}\left(\frac{\beta l}{2}\right)^3\right]\right\}\end{aligned} \tag{7}$$

where

$$\beta=\omega\sqrt{\frac{m}{T_0}} \tag{8}$$

As the effects of cable sag on the efficiency of transverse dampers are mainly in the first mode (Xu and Yu 1998, Krenk and Nielsen 2002, Johnson *et al*. 2003, Duan 2004, Christenson *et al*. 2006, Wang *et al.* 2018), only nearly symmetric vibrations of the cable are considered in this study. The nearly symmetric vibrations are associated with the second factor in Eq. (7). By dividing $\sin(\beta l/2)$ on both sides of Eq. (7) to remove the roots associated with the nearly antisymmetric modes, the wave numbers determinant equation of nearly symmetric vibrations is derived as

$$\left\{\tan\left(\frac{\beta l}{2}\right)-\left[\frac{\beta l}{2}-\frac{4}{\lambda^2}\left(\frac{\beta l}{2}\right)^3\right]\right\}(1+2\Phi\Theta)=2\Phi\tan\left(\frac{\beta l}{2}\right)\Theta^2\left[\frac{\beta l}{2}-\frac{4}{\lambda^2}\left(\frac{\beta l}{2}\right)^3\right] \tag{9}$$

where Φ reflects the effect of the IMD force with the expression as

$$\Phi=\frac{1}{\beta T_0}\frac{\tilde{F}_{\mathrm{IMD}}}{\tilde{y}_{\mathrm{d}}}=\frac{-m_e\omega^2+c_{\mathrm{eq}}i\omega}{\beta T_0} \tag{10}$$

and Θ is defined as

$$\Theta=\frac{\sin\left(\frac{\beta x_{\mathrm{d}}}{2}\right)\sin\left(\frac{\beta x_{\mathrm{d}}'}{2}\right)}{\sin\left(\frac{\beta l}{2}\right)} \tag{11}$$

The equation solving for tan ($\beta l/2$) is subsequently derived as

$$\tan\left(\frac{\beta l}{2}\right)=\left[\frac{\beta l}{2}-\frac{4}{\lambda^2}\left(\frac{\beta l}{2}\right)^3\right]+\frac{2\Phi\Theta^2\left[\frac{\beta l}{2}-\frac{4}{\lambda^2}\left(\frac{\beta l}{2}\right)^3\right]^2}{1+2\Phi\Theta\left\{1\text{-}\Theta\left[\frac{\beta l}{2}-\frac{4}{\lambda^2}\left(\frac{\beta l}{2}\right)^3\right]\right\}} \tag{12}$$

2.2 Numerical solution

The numerical solution can be obtained from Eq. (12) by the fixed-point iteration, where the iterative scheme is

.

$$\beta_n^{j+1}l=(n+1)\pi+2\arctan\left\{\left[\frac{\beta_n^j l}{2}-\frac{4}{\lambda^2}\left(\frac{\beta_n^j l}{2}\right)^3\right]+\frac{2\Phi\Theta\left(\beta_n^j\right)^2\left[\frac{\beta_n^j l}{2}-\frac{4}{\lambda^2}\left(\frac{\beta_n^j l}{2}\right)^3\right]^2}{1+2\Phi\Theta\left(\beta_n^j\right)\left\{1\text{-}\Theta\left(\beta_n^j\right)\left[\frac{\beta_n^j l}{2}-\frac{4}{\lambda^2}\left(\frac{\beta_n^j l}{2}\right)^3\right]\right\}}\right\} \tag{13}$$

The process starts from the undamped wave number of the n^{th} mode β_n^0, which can be obtained by substituting $\tilde{F}_{\mathrm{IMD}}=0$ into Eq. (12)

$$\tan\left(\frac{\beta_n^0 l}{2}\right)=\left[\frac{\beta_n^0 l}{2}-\frac{4}{\lambda^2}\left(\frac{\beta_n^0 l}{2}\right)^3\right] \tag{14}$$

After solving the wave number of the n^{th} mode β_n, the corresponding eigen frequency of the n^{th} mode ω_n can be calculated by Eq. (8). The eigen frequency related to the modal damping ratio can be expressed as

$$\omega_n=|\omega_n|\left(\sqrt{1-\zeta_n^2}+i\zeta_n\right) \tag{15}$$

where ζ_n is the n^{th} modal damping ratio of the cable.

Therefore, the n^{th} modal damping ratio of the cable can be finally determined as

$$\zeta_{\mathrm{n}} = \frac{\mathrm{Im}(\omega_n)}{|\omega_n|} = \frac{\mathrm{Im}(\beta_n l)}{|\beta_n l|} \tag{16}$$

2.3 Asymptotic solution

The asymptotic solution for a sag cable with a passive viscious damper has been well developed (Krenk and Nielsen 2002, Duan 2004). To facilitate the optimal design of the IMD, this section extends their studies to derive the asymptotic solution of a sag cable with an IMD. The solution is established on the assumptions that the IMD is installed close to the cable end ($x_d << l$), and the installation of the IMD causes minimal perturbation in the wave numbers ($\beta_n - \beta_n^0 << \beta_n^0$).

Rewrite Eq. (9) as

$$\tan(\frac{\beta l}{2}) - [\frac{\beta l}{2} - \frac{4}{\lambda^2}(\frac{\beta l}{2})^3] = \frac{2\Phi\left[\frac{\sin(\frac{\beta x_\mathrm{d}}{2})\sin(\frac{\beta x'_\mathrm{d}}{2})}{\cos(\frac{\beta l}{2})}\right]^2 [\frac{\beta l}{2} - \frac{4}{\lambda^2}(\frac{\beta l}{2})^3]}{\tan(\frac{\beta l}{2}) + 2\Phi\left[\frac{\sin(\frac{\beta x_\mathrm{d}}{2})\sin(\frac{\beta x'_\mathrm{d}}{2})}{\cos(\frac{\beta l}{2})}\right]^2} \tag{17}$$

The left-hand of the Eq. (17) can be linearized around the undamped value $\beta_n^0 l$

$$\tan(\frac{\beta l}{2}) - [\frac{\beta l}{2} - \frac{4}{\lambda^2}(\frac{\beta l}{2})^3] \approx \tan(\frac{\beta_n^0 l}{2}) - [\frac{\beta_n^0 l}{2} - \frac{4}{\lambda^2}(\frac{\beta_n^0 l}{2})^3] + \left[\tan^2(\frac{\beta_n^0 l}{2}) + \frac{12}{\lambda^2}(\frac{\beta_n^0 l}{2})^2\right]\frac{\beta_n l - \beta_n^0 l}{2} \tag{18}$$

Substituting Eq. (14) and Eq. (18) into Eq. (17) and using the following relation

$$\frac{\sin(\frac{\beta x_\mathrm{d}}{2})\sin(\frac{\beta x'_\mathrm{d}}{2})}{\cos(\frac{\beta l}{2})} = \sin(\beta x_\mathrm{d})\tan(\beta l)\left[1 - \frac{\tan(\frac{\beta x_\mathrm{d}}{2})}{\tan(\frac{\beta l}{2})}\right] \tag{19}$$

we can obtain

$$\beta_n l - \beta_n^0 l = \frac{\Phi \sin^2(\beta_n^0 x_\mathrm{d})\left[1 - \frac{\tan(\frac{\beta_n^0 x_\mathrm{d}}{2})}{\tan(\frac{\beta_n^0 l}{2})}\right]^2 \tan^2(\frac{\beta_n^0 l}{2})}{\left\{1 + \Phi \sin(\beta_n^0 x_\mathrm{d})\left[1 - \frac{\tan(\frac{\beta_n^0 x_\mathrm{d}}{2})}{\tan(\frac{\beta_n^0 l}{2})}\right]\right\}\left[\tan^2(\frac{\beta_n^0 l}{2}) + \frac{12}{\lambda^2}(\frac{\beta_n^0 l}{2})^2\right]} \tag{20}$$

Given that $x_d << l$ and $\beta_n - \beta_n^0 << \beta_n^0$, we can achieve the following approximations

$$\left[1 - \frac{\tan(\frac{\beta_n^0 x_\mathrm{d}}{2})}{\tan(\frac{\beta_n^0 l}{2})}\right] \approx 1, \quad \sin(\beta_n^0 x_\mathrm{d}) \approx \beta_n^0 x_\mathrm{d} \tag{21}$$

By substituting Eq. (21) into Eq. (20), the Eq. (20) can be simplified as

$$\Delta\beta_n = \left(\beta_n - \beta_n^0\right) = \frac{\beta_n^{\ 0} x_\mathrm{d}(-m_\mathrm{e}\omega_n^2 + c_\mathrm{eq} i\omega_n)}{T_0 + x_\mathrm{d}(-m_\mathrm{e}\omega_n^2 + c_\mathrm{eq} i\omega_n)}\frac{x_\mathrm{d}}{l}\frac{1}{\left[\tan^2(\frac{\beta_n^0 l}{2}) + \frac{12}{\lambda^2}\left(\frac{\beta_n^0 l}{2}\right)^2\right] / \tan^2(\frac{\beta_n^0 l}{2})} \tag{22}$$

The modal damping ratios of the cable can be obtain by

$$\zeta_n = \frac{\mathrm{Im}(\Delta\beta_n)}{|\beta_n^0|} = \frac{c_\mathrm{eq}\omega_n T_0 x_\mathrm{d}}{(T_0 - m_\mathrm{e}\omega_n^2 x_\mathrm{d})^2 + (c_\mathrm{eq}\omega_n x_\mathrm{d})^2}\frac{1}{W_{\lambda^2}}\frac{x_\mathrm{d}}{l} \tag{23}$$

where W_{λ^2} is the damping ratio modification factor due to sag of a passive viscous damper

$$W_{\lambda^2} = [\tan^2(\frac{\beta_n^0 l}{2}) + \frac{12}{\lambda^2}(\frac{\beta_n^0 l}{2})^2] / \tan^2(\frac{\beta_n^0 l}{2}) \tag{24}$$

where W_{λ^2} is larger than 1 when $\lambda^2 > 0$.

By introducing the following dimensionless parameters as

$$\bar{m}_{\mathrm{e},n} = \varphi_k \bar{m}_{\mathrm{e},n}^{\mathrm{T}}, \quad \eta_n = \varphi_c \frac{\omega_n^{0,T} c_\mathrm{eq}}{T_0}\frac{x_\mathrm{d}}{(1\text{-}\bar{m}_{e,n})}, \quad \bar{m}_{\mathrm{e},n}^{\mathrm{T}} = m_\mathrm{e}(\omega_n^{0,T})^2 x_\mathrm{d} / T_0 \tag{25}$$

the modal damping ratios of the cable can be subsequently derived as

$$\zeta_n = \frac{1}{1\text{-}\varphi_k \bar{m}_{\mathrm{e},n}^{\mathrm{T}}}\frac{\eta_n}{1+\eta_n^2}\frac{1}{W_{\lambda^2}}\frac{x_\mathrm{d}}{l} \tag{26}$$

where $\bar{m}_{e,n}$ and η_n denote the dimensionless inertial mass and the dimensionless damping coefficient of the IMD for the n^{th} mode of the cable with sag, $\bar{m}_{\mathrm{e},n}^{\mathrm{T}}$ denotes the dimensionless inertial mass of the IMD for the n^{th} mode of the taut cable, $\omega_n^{0,T}$ is the undamped frequency of a taut cable, φ_k and φ_c are the modification factor of the inertial mass and the damping coefficient due to the sag, respectively

$$\varphi_k = (\frac{\beta_n^0 l}{n\pi})^2, \quad \varphi_c = \frac{\beta_n^0 l}{n\pi} \tag{27}$$

The optimum damping coefficient $c_{\mathrm{eq},n}^{\mathrm{opt}}$ corresponding to a constant m_e can be obtained by

$$\frac{\partial \zeta_n}{\partial c_\mathrm{eq}} = 0 \tag{28}$$

leading the value

$$c_{\mathrm{eq},n}^{\mathrm{opt}} = \left|1\text{-}\varphi_\mathrm{k}\bar{m}_{\mathrm{e},n}^{\mathrm{T}}\right|\frac{T_0}{\varphi_\mathrm{c} x_\mathrm{d}\omega_n^{0,T}} \tag{29}$$

The corresponding optimal damping ratio in the cable n^{th} mode can be obtained as

$$\zeta_n^{\mathrm{opt}} = \frac{1}{(1-\varphi_k \bar{m}_{\mathrm{e},n}^{\mathrm{T}})W_{\lambda^2}}\frac{x_\mathrm{d}}{2l} \tag{30}$$

Table 1 The main properties of the test model cables

Cable with small sag		Cable with large sag	
Item	Value	Item	Value
Cable length (l)	11.4 m	Cable length (l)	11.4 m
Cross-section area (A)	1.374 cm^2	Cross-section area (A)	1.374 cm^2
Mass per unit length (m)	15.0 kg/m	Mass per unit length (m)	9.5 kg/m
Elasticity modulus (E)	200 GPa	Elasticity modulus (E)	200 GPa
Tension force (T_0)	44.0 kN	Tension force (T_0)	19.2 kN
Inclination angle (θ)	0°	Inclination angle (θ)	0°
Sag parameter(λ^2)	0.906	Sag parameter(λ^2)	4.513
The first modal natural frequency	2.55 Hz	The first modal natural frequency	2.25Hz

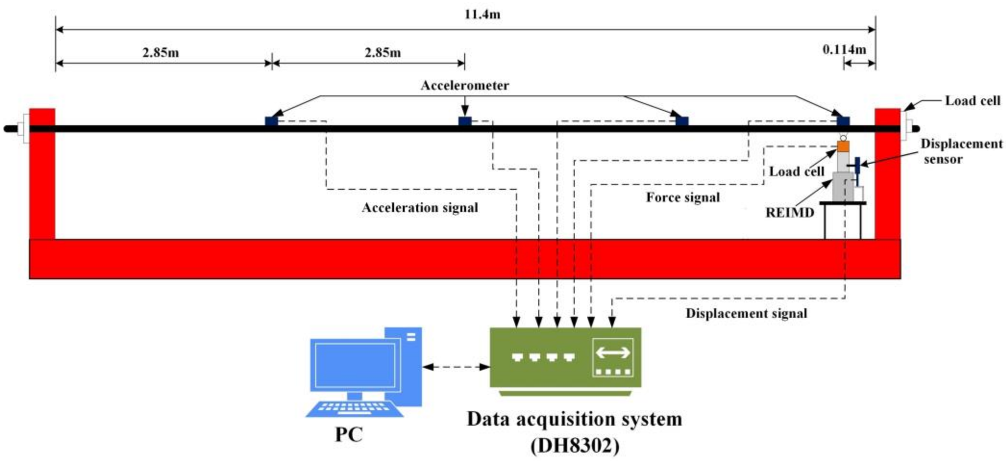

Fig. 2 Schematic diagram of test setup for cable vibration control

As the cable sag always increases the undamped frequency of the cable (Krenk and Nielsen 2002, Johnson *et al.* 2003, Duan 2004), φ_k and φ_c are greater than 1 when $\lambda^2 > 0$. Hence, the cable sag tends to decrease the optimal damping coefficient of the IMD and the following equation is satisfied

$$\zeta_n^{\mathrm{opt}} = \frac{1}{(1-\varphi_k \bar{m}^{\mathrm{T}}_{\mathrm{e},n})W_{\lambda^2}} \frac{x_{\mathrm{d}}}{2l} > \frac{1}{(1-\bar{m}^{\mathrm{T}}_{\mathrm{e},n})W_{\lambda^2}} \frac{x_{\mathrm{d}}}{2l} \quad \text{when } \varphi_k \bar{m}^{\mathrm{T}}_{\mathrm{e},n} < 1 \tag{31}$$

which means the IMD tends to alleviate the negative effect induced by the cable sag compared with the passive viscous damper when the $\varphi_k \bar{m}^{\mathrm{T}}_{\mathrm{e},n}$ is less than unity. In addition, when

$$\zeta_n^{\mathrm{opt}} = \frac{1}{(1-\varphi_k \bar{m}^{\mathrm{T}}_{\mathrm{e},n})W_{\lambda^2}} \frac{x_{\mathrm{d}}}{2l} > \frac{1}{(1-\bar{m}^{\mathrm{T}}_{\mathrm{e},n})} \frac{x_{\mathrm{d}}}{2l} \tag{32}$$

the cable with sag tends to increase maximum modal damping ratios provided by the IMD compared with taut cable. Here, the dimensionless inertial mass falls in the range of

$$(W_{\lambda^2}-1)/(\varphi_k W_{\lambda^2}-1) < m^{\mathrm{T}}_{\mathrm{e},n} < 1/\varphi_k \tag{33}$$

3. Experiment investigation of a sag cable with an EIMD

3.1 Experimental setup

To experimentally evaluate the impact of cable sag on the efficiency of an IMD in controlling stay cable vibrations and validate theoretical analysis results above, two model cables with different dynamic characteristics and sag parameters were established in the laboratory. The main properties of the model cables are listed in Table 1. Fig. 2 illustrates schematic diagram of test setup for cable vibration control, and corresponding photos are shown in Fig. 3. An electromagnetic IMD (EIMD) shown in Fig. 3 (b) was attached transversely to the cable at 0.114 m (i.e., 1% of the cable length) away from the right anchorage, incorporating a load cell and a displacement sensor to monitor the mechanical performance of the EIMD. Three accelerator-meters were installed at two quarter-spans and the mid-span of the cable to monitor the cable acceleration responses, which were adopted to identify the modal damping ratios of the cable. All the signals were collected by the DH8302 data acquisition system with 200 Hz sampling frequency.

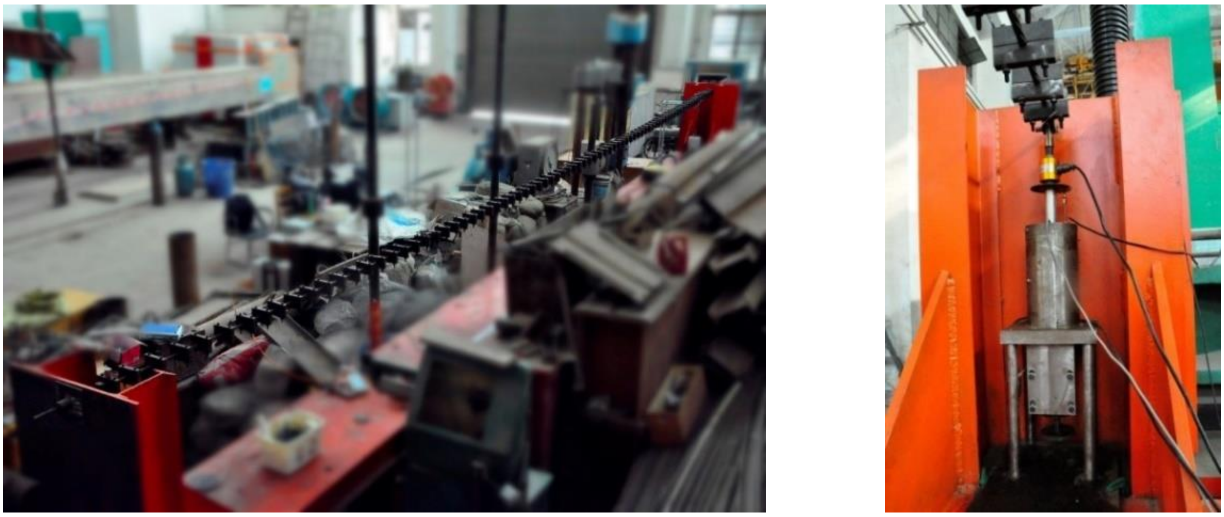

(a) Test cable (b) EIMD

Fig. 3 Test photos of cable vibration control

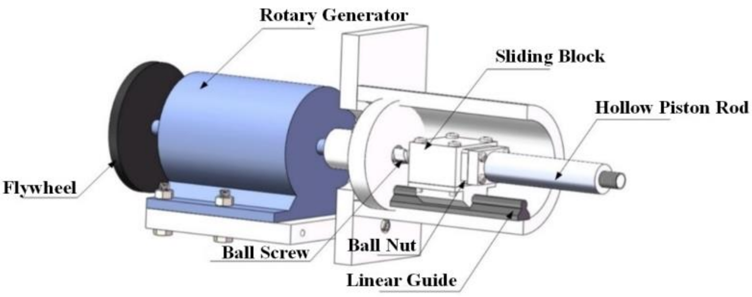

Fig. 4 Schematic diagram of an EIMD

Table 2 Design parameters of the EIMD

Components	Parameters	Values
Rotary generator	Electromotive force constant	$0.06V/(r \cdot min^{-1})$
	Maximum angular velocity	3000r/min
	Internal resistance	6.4Ω
	Load resistance	40Ω, 80Ω
Ball screw	Diameter	16 mm
	Lead	16 mm
Flywheel	Diameter-thickness (#1)	9.0 cm-1.0 cm
	Diameter-thickness (#2)	11.0 cm-1.0 cm
	Diameter-thickness (#3)	13.0 cm-1.0 cm
	Diameter-thickness (#4)	15.5 cm-1.0 cm
	Diameter-thickness (#5)	19.0 cm-1.0 cm

3.2 EIMD

An EIMD with adjustable inertial mass was developed to mitigate the model cables vibrations. The design parameters of the EIMD are given in Table 2. The EIMD, shown in Fig. 4, mainly consists of a rotary generator, a ball screw, a flywheel and a liner guide way. The linear motion of the cable can be converted into the high-speed rotational motion of the rotary generator and the flywheel through the ball screw amplification mechanism. A magnified axial initial force and damping force of the EIMD are generated by the rotational flywheel and the generator, respectively.

Table 3 The identified inertial mass and damping coefficient of the EIMD

EIMD	Cable with small sag					Cable with large sag				
	m_e (kg)	$\bar{m}^T_{e,1}$	$\bar{m}_{e,1}$	c_{eq} (Ns/m) 40Ω	c_{eq} (Ns/m) 80Ω	m_e (kg)	$\bar{m}^T_{e,1}$	$\bar{m}_{e,1}$	c_{eq} (Ns/m) 40Ω	c_{eq} (Ns/m) 80Ω
without flywheel	103.2	0.060	0.069	4047	3080	102.6	0.093	0.122	4659	3117
with #1 flywheel	153.2	0.088	0.102	4352	3192	140.5	0.128	0.167	4778	3177
with #2 flywheel	279.2	0.161	0.186	4847	3300	259.7	0.236	0.308	4636	3087
with #3 flywheel	461.3	0.266	0.307	4561	3083	422.0	0.384	0.500	4968	3197
with #4 flywheel	851.4	0.491	0.611	4326	3248	808.1	0.736	0.958	4639	3017
with #5 flywheel	1775.7	1.024	1.180	4041	3272	1684.5	1.534	1.997	4719	3028

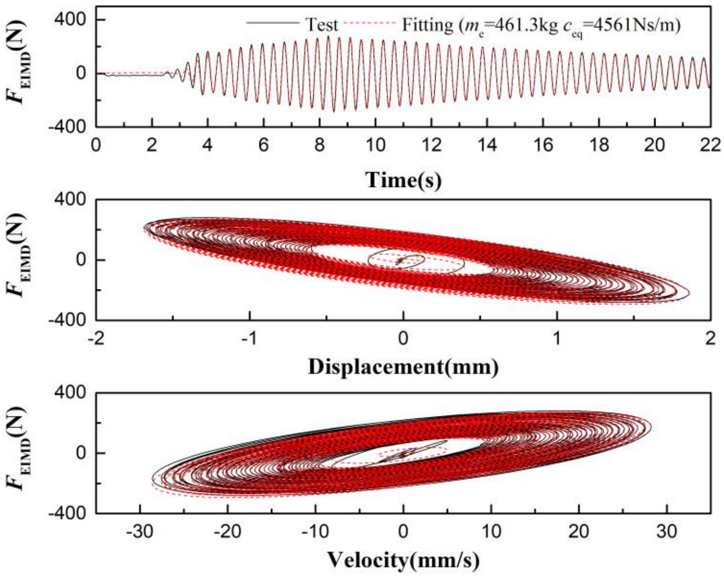

Fig. 5 Comparison between the fitting and experimentally obtained responses (cable with small sag, EIMD with #3 flywheel, load resistance: 40Ω)

The inertial mass and the equivalent damping coefficient of the EIMD can be identified by the least square method according to the measured displacement and the force of the EIMD based on the mechanical model of the EIMD [i.e., Eq. (1)]. The identified parameters of the EIMD are summarized in Table 3, and comparisons shown in Fig. 5 demonstrate the feasibility of the model.

3.3 Experimental results and discussion

Series of free vibration tests were conducted to evaluate the mitigation performance of the cable with the EIMD. Each cable was excited manually at its first modal natural frequency, where the excitation position was located at 0.25*l* away from the left anchorage of the cable. The typical time history responses of accelerations at the mid-span of each cable in the first mode are shown in Figs. 6 and 7. An exponential function is utilized to fit the envelope curve of the free decay responses to identify modal damping ratios of two cables. Since modal damping ratios may depend on the amplitudes of cable vibrations, the interval accelerations of 6-10 m/s^2 and 4-8 m/s^2 are selected to identify modal damping ratios of the cable with small sag and large sag, respectively.

As can be seen from Figs. 6 and 7, the uncontrolled first modal damping ratios of the cable with small sag and large sag are 0.14% and 0.22%, respectively. The electromagnetic damper (an EIMD without a flywheel) that is similar to a passive viscous damper increases cables damping ratio to 0.28% and 0.45%, respectively. For the EIMD with #3 flywheel or #4 flywheel, the first modal damping ratio of the cable with small sag is increased to 0.42% or 0.62%, while the first modal damping ratio of the cable with large sag is increased to 0.70% or 1.23%, respectively. It is shown that the achievable first modal damping ratios of the cable with the EIMD are superior to those with the electromagnetic damper (passive viscous damper), which demonstrates that the inertial mass of the EIMD is beneficial to improve control performance of the cable with sag.

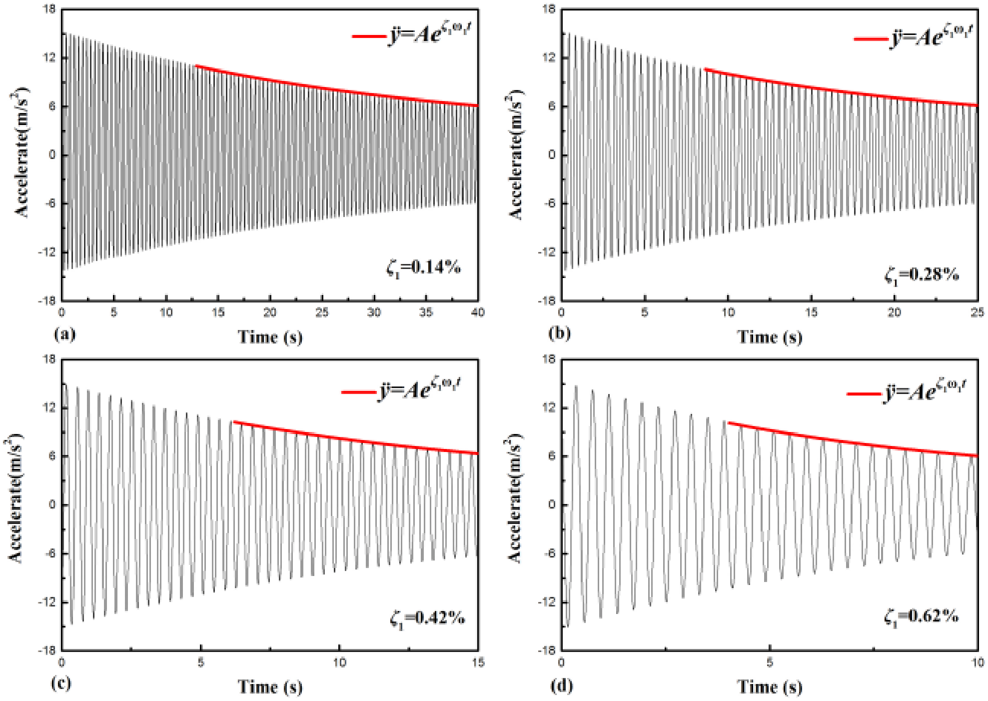

Fig. 6 Time history responses of accelerations at mid-span of the cable with small sag in the first mode: (a) without control, (b) EIMD without flywheel, (c) EIMD with #3 flywheel and (d) EIMD with #4 flywheel

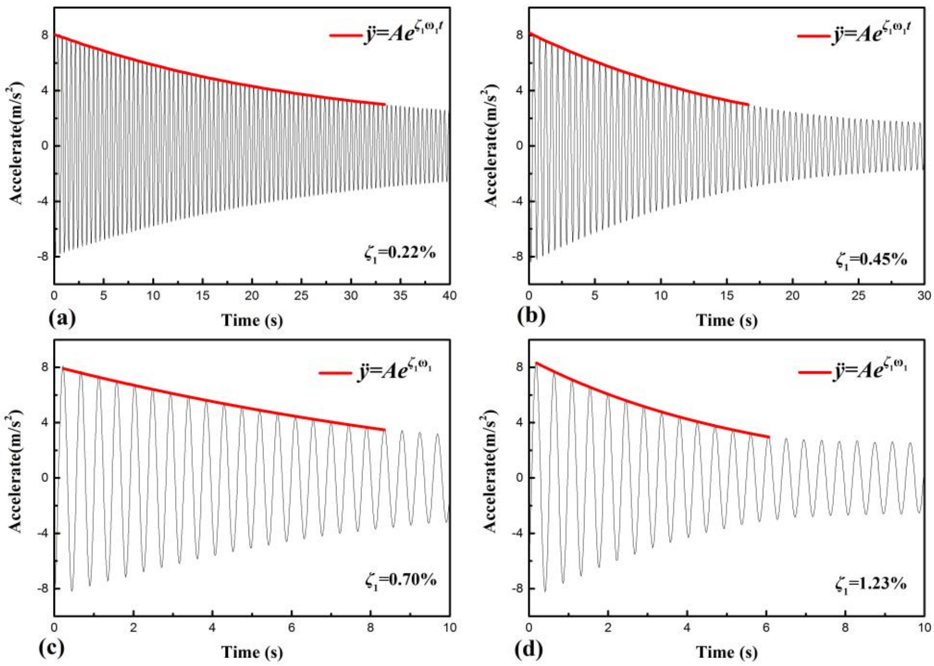

Fig. 7 Time history responses of accelerations at mid-span of the cable with large sag in the first mode: (a) without control, (b) EIMD without flywheel, (c) EIMD with #3 flywheel and (d) EIMD with #4 flywheel

Figs. 8 and 9 give the comparison between the theoretical and the experimental supplemental modal damping ratios in the first mode of the cable with small and large sag, respectively. Corresponding results are summarized in Table 4 and Table 5, respectively. The comparison results demonstrate that the asymptotic solution agrees with the numerical solution well when small or moderate inertial mass is used in the EIMD, shown in Figs. 8(a)-8(e) and Figs. 9(a)-9(d). However, the asymptotic solution will deviate from the numerical solution when larger inertial mass is adopted in the EIMD, shown in Fig. 8(f) and Figs. 9(e)-9(f). This is mainly because the assumption $\beta_n - \beta_n^0 \ll \beta_n^0$ for the asymptotic solution is no longer satisfied when large inertial mass is used in the IMD (Shi and Zhu 2018, Wang *et al*. 2018).

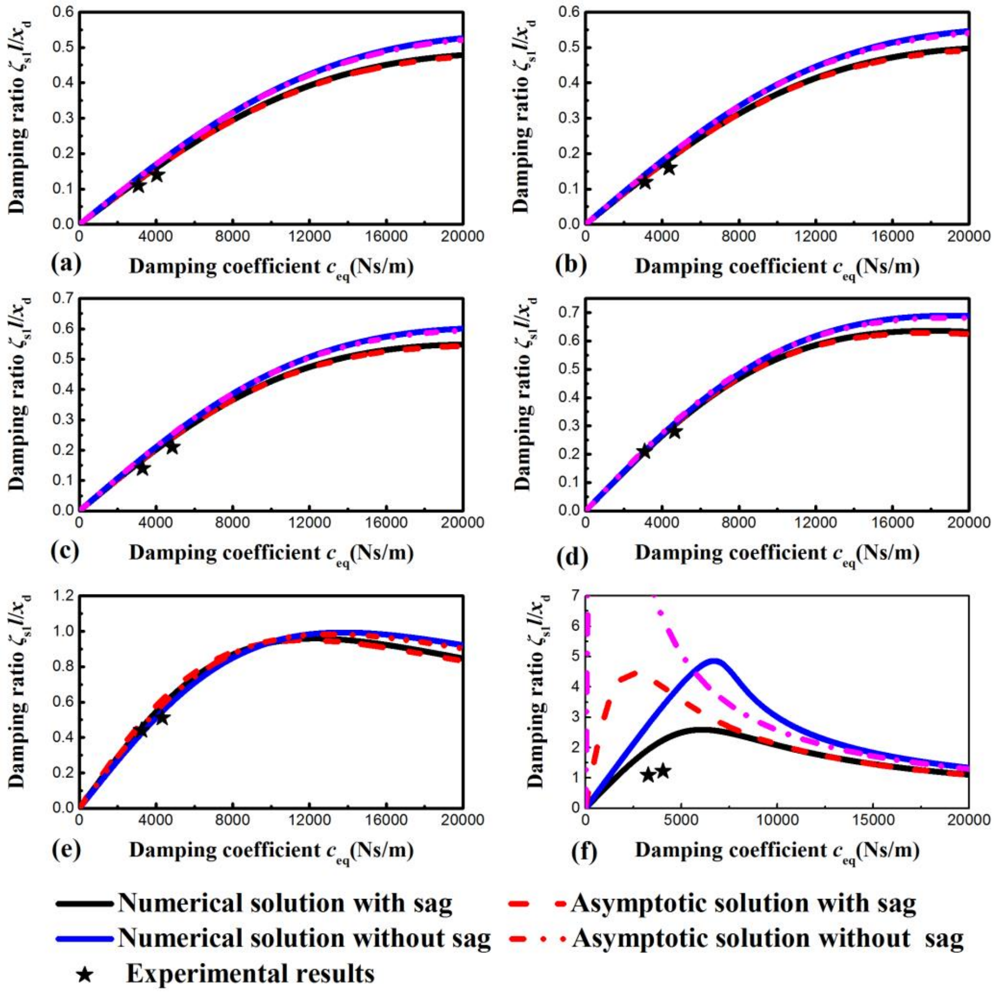

Fig. 8 Comparison between experimental and theoretical damping ratios in the first mode of the cable with small sag: (a) without flywheel, (b) with #1 flywheel, (c) with #2 flywheel, (d) with #3 flywheel, (e) with #4 flywheel and (f) with #5 flywheel

Table 4 Theoretical and experimental supplemental modal damping ratios of the cable with small sag

EIMD	Cable with sag (%)				Cable without sag (%)				Experimental results (%)	
	num. results		asy. results		num. results		asy. results			
	40Ω	80Ω	40Ω	80Ω	40Ω	80Ω	40Ω	80Ω	40Ω	80Ω
without flywheel	0.16	0.12	0.16	0.12	0.17	0.13	0.17	0.13	0.14	0.11
with #1 flywheel	0.18	0.14	0.18	0.14	0.20	0.15	0.20	0.15	0.16	0.12
with #2 flywheel	0.24	0.17	0.24	0.17	0.25	0.18	0.25	0.18	0.21	0.14
with #3 flywheel	0.30	0.21	0.31	0.21	0.31	0.21	0.32	0.22	0.28	0.21
with #4 flywheel	0.58	0.46	0.61	0.49	0.55	0.42	0.58	0.46	0.51	0.44
with #5 flywheel	2.25	1.94	3.98	4.29	3.02	2.48	6.24	7.61	1.22	1.09

For the cable with small sag, theoretical modal damping ratios (including numerical and asymptotic solutions) taking into account the cable sag are slightly smaller than those without cable sag effect, and more closer to the experimental results except for the EIMD with #5 flywheel. For the cable with large sag, theoretical modal damping ratios taking into account the cable sag generally agree well with the experimental results except for the EIMD with the #4 flywheel or the #5 flywheel. It is shown that theoretical results neglecting the cable sag effect significantly overestimate the achievable first modal damping ratios of the cable. It is also worth noting that both the numerical and asymptotic solutions of the cable with small sag or large sag lose their accuracies when the EIMD adopts lager inertial mass.

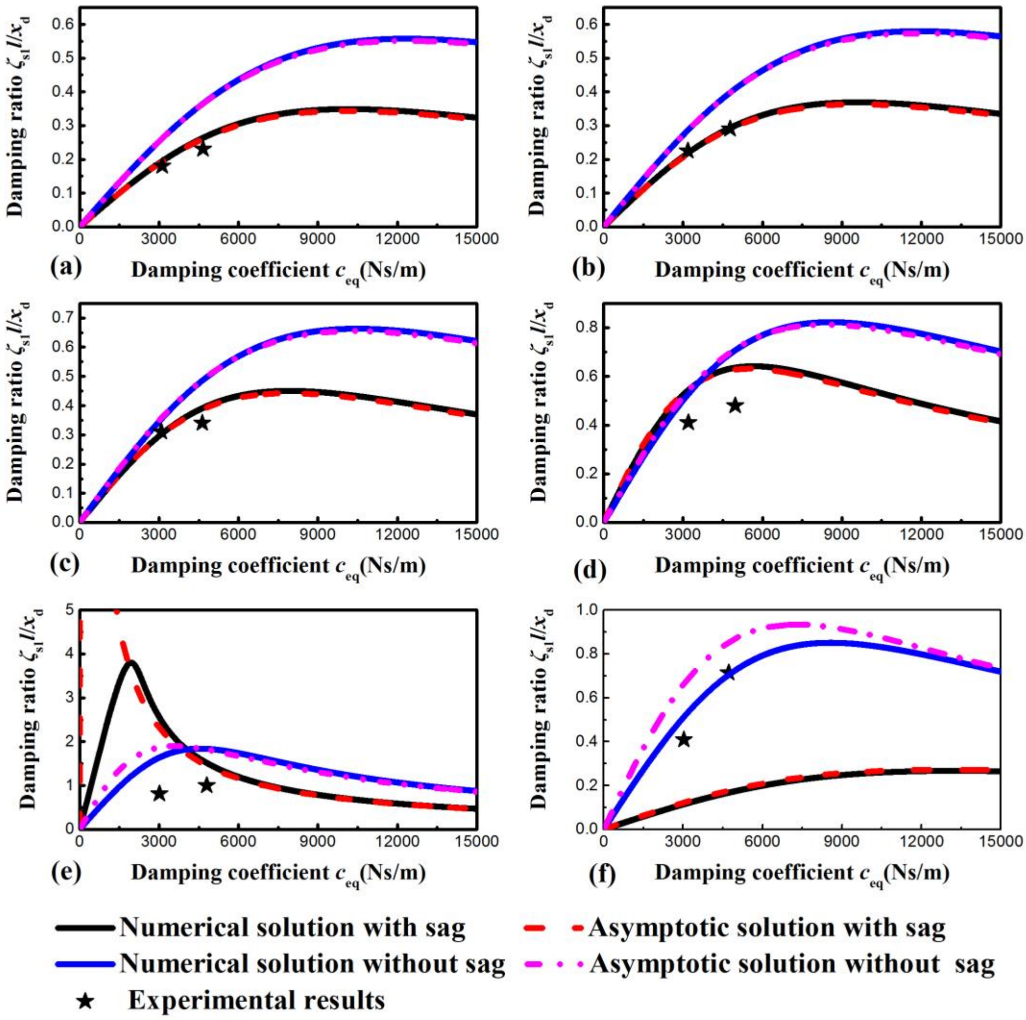

Fig. 9 Comparison between experimental and theoretical damping ratios in the first mode of the cable with largesag: (a) without flywheel, (b) with #1 flywheel, (c) with #2 flywheel, (d) with #3 flywheel, (e) with #4 flywheel and (f) with #5 flywheel

Table 5 Theoretical and experimental supplemental modal damping ratios of the cable with large sag

EIMD	Cable with sag (%)				Cable without sag (%)				Experimental results (%)	
	num. results		asy. results		num. results		asy. results			
	40Ω	80Ω	40Ω	80Ω	40Ω	80Ω	40Ω	80Ω	40Ω	80Ω
without flywheel	0.26	0.19	0.26	0.19	0.37	0.26	0.37	0.26	0.23	0.18
with #1 flywheel	0.29	0.22	0.29	0.22	0.39	0.29	0.40	0.29	0.28	0.23
with #2 flywheel	0.39	0.30	0.39	0.30	0.49	0.35	0.49	0.36	0.35	0.31
with #3 flywheel	0.64	0.54	0.63	0.55	0.71	0.53	0.71	0.54	0.48	0.41
with #4 flywheel	1.57	2.55	1.50	2.31	1.84	1.64	1.83	1.87	1.01	0.82
with #5 flywheel	0.17	0.11	0.18	0.12	0.70	0.51	0.85	0.66	0.72	0.41

Similar to passive viscous dampers, the cable sag generally decreases supplemental modal damping ratios of the cable. However, as shown in Figs. 8 and Fig. 9, the supplemental modal damping ratios differences with or without considering the cable sag effect become smaller with the increase of the inertial mass of the IMD, which means the IMD tends to alleviate the negative effect induced by the cable sag. In addition, the optimum damping coefficient of the IMD for a sag cable is less than that for a taut cable when corresponding achievable damping ratio of the cable increases with the increase of the inertial mass of the IMD, which implies that the cable sag will decrease the optimum damping coefficient of the IMD when the inertial mass is not exceed its optimal value.

4. Conclusions

It has been theoretically predicted that superior supplemental damping can be generated for a taut cable with an IMD. This paper extends previous studies to investigate the effect of the cable sag on the efficiency of an IMD in controlling stay cable vibrations, theoretically and experimentally. The main conclusions are summarized as follows:

(1) The theoretical analysis indicates that the cable sag generally reduces the first modal damping ratios provided by the IMD. Unlike the passive viscous damper, the IMD tends to alleviate the negative effect induced by the cable sag since the cable sag can increase the dimensionless inertial mass of the IMD. In addition, the cable sag decreases the optimum damping coefficient when the dimensionless inertial mass is less than an optimal value.

(2) Both the theoretical and experimental results demonstrate that the IMD can provide superior damping to a cable. The first modal damping ratio of a sag cable with an IMD will be significantly overestimated with a taut-cable model, especially for the cable with large sag. After taking into account the cable sag, theoretical modal damping ratios of the cable predicted by both numerical solution and asymptotic solution generally agree well with experimental results. Special attentions should be paid to cable sag effect in the design of the IMD for cable vibration control.

Acknowledgments

The authors greatly acknowledge the financial suppo rt from the National Natural Science Foundation of Chi na (Grant No. 51878274 and 51778228) and National B asic Research Program of China (973 Program) (Grant No. 2015CB060000 and 2015CB057702).

References

Ahmad, J., Cheng, S.H. and Ghrib, F. (2018), "Combined effect of external damper and cross-tie on the modal response of hybrid two-cable networks", *J. Sound Vib.*, **417**, 132-148. https://doi.org/10.1016/j.jsv.2017.12.023.

Cai, C.S., Wu, W.J. and Araujo, M. (2007), "Cable vibration control with a TMD-MR damper system: experimental exploration", *J. Struct. Eng.-ASCE*, **133**(5), 629-637. https://doi.org/10.1061/(ASCE)0733-9445(2007)133:5(629).

Chen, L., Sun, L.M. and Nagarajaiah, S. (2015), "Cable with discrete negative stiffness device and viscous damper: passive realization and general characteristics", *Smart Struct. Syst.*, **15**(3), 627-643. http://dx.doi.org/10.12989/sss.2015.15.3.627.

Chen, Z.Q., Wang, X.Y., Ko, J.M., *et al.* (2004), "MR damping system for mitigating wind-rain induced vibration on Dongting Lake Cable-Stayed Bridge", *Wind Struct.*, **7**(5), 293-304. http://dx.doi.org/10.12989/was.2004.7.5.293.

Christenson, R.E., Spencer, B.F. and Johnson, E.A. (2006), "Experimental verification of smart cable damping", *J. Eng. Mech.-ASCE*, **132**(3), 268-278. https://doi.org/10.1061/(ASCE)0733-9399(2006)132:3(268).

Cu, V.H., Han, B., Pham, D.H., *et al.* (2018), "Free vibration and damping of a taut cable with an attached viscous mass damper", *KSCE J. Civ. Eng.*, **22**(5), 1792-1802.

Duan, Y.F. (2004), "Vibration control of stay cables using semi-active magneto-rheological (MR) dampers", Ph.D. Dissertation, The Hong Kong Polytechnic University, Hong Kong.

Duan, Y.F., Ni, Y.Q. and Ko, J.M. (2006), "Cable vibration control using magneto-rheological (MR) dampers", *J. Intel. Mat. Syst. Str.*, **17**(4), 321-325. https://doi.org/10.1142/9789812702197_0121.

Fournier, J.A. and Cheng, S.H. (2014), "Impact of damper dtiffness and damper support stiffness on the efficiency of a linear viscous damper in controlling stay cable vibrations", *J. Bridge Eng.*, 2014, **19**(4), 04013022.

Fujino, Y. and Hoang, N. (2008), "Design formulas for damping of a stay cable with a damper", *J. Bridge Eng.*, **134**(2), 269-278. https://doi.org/10.1061/(ASCE)0733-9445(2008)134:2(269).

He, X.H., Cai, C., Wang, Z.J., *et al.* (2018), "Experimental verification of the effectiveness of elastic cross-ties in suppressing wake-induced vibrations of staggered stay cables", *Eng. Struct.*, **167**, 151-165. https://doi.org/10.1016/j.engstruct.2018.04.033.

Huang, H., Sun, L.M. and Jiang, X. (2012), "Vibration mitigation of stay cable using optimally tuned MR damper", *Smart Struct. Syst.*, **9**(1), 35-53.

Ikago, K., Saito, K. and Inoue, N. (2012), "Seismic control of single-degree-of-freedom structure using tuned viscous mass damper", *Earthq. Engng. Struct. D.*, **41**(3), 453-474. https://doi.org/10.1002/eqe.1138.

Irvine, H.M. and Caughey, T.K. (1974), "The linear theory of free vibrations of a suspended cable", *Proc. R. Soc. Lond. A*, **341**, 299-315. https://doi.org/10.1098/rspa.1974.0189.

Johnson, E.A., Christenson, R.E. and Spencer, B.F. (2003), "Semi-active damping of cables with sag", *Comput.-Aided. Civ. Inf.*, **18**(2), 132-146. https://doi.org/10.1111/1467-8667.00305.

Jung, H.J., Jang, J.E., Choi, K.M., *et al.* (2008), "MR fluid damper-based smart damping systems for long steel stay cable under wind load", *Smart. Struct. Syst.*, **4**(5), 697-710.

Kim, I.H., Jung, H.J. and Koo, J.H. (2010), "Experimental evaluation of a self-powered smart damping system in reducing vibration of a full-scale stay cable", *Smart Mater. Struct.*, **19**, 115027(1-10).

Krenk, S. (2000). "Vibrations of a taut cable with an external damper", *J. Appl. Mech.*, **67**(4), 772-776. doi:10.1115/1.1322037.

Krenk, S. and Nielsen, S.R.K. (2002), "Vibrations of a shallow cable with a viscous damper", *Proc. R. Soc. Lond. A*, **458**, 339-357. *https://doi.org/10.1098/rspa.2001.0879*.

Lazar, I.F., Neild, S.A. and Wagg, D.J. (2016), "Vibration suppression of cables using tuned inerter dampers", *Eng. Struct.*, **122**, 62-71. https://doi.org/10.1016/j.engstruct.2016.04.017.

Li, H., Liu, M., Li, J.H., *et al*. (2007), "Vibration control of stay cables of Shandong Binzhou Yellow River Highway Bridge by using magnetorheological fluid dampers", *J. Bridge Eng.-ASCE*, **12**(4), 401-409. https://doi.org/10.1061/(ASCE)1084-0702(2007)12:4(401).

Li, H., Liu, M. and Ou, J.P. (2008), "Negative stiffness characteristics of active and semi-active control systems for stay cables", *Struct. Control Health Monit.*, **15**(2), 120-142. https://doi.org/10.1002/stc.200.

Lu, L., Duan, Y.F., Spencer, B.F., *et al.* (2017), "Inertial mass damper for mitigating cable vibration", *Struct. Control Health Monit.*, **24**(10), 1-12. https://doi.org/10.1002/stc.1986.

Luo, J.N., Jiang, J.Z. and Macdonald, J.H.G. (2019), "Cable vibration suppression with inerter-based absorbers", *J. Eng. Mech.*, **145**(2), 04018134. https://doi.org/10.1061/(ASCE)EM.1943-7889.0001554.

Nakamura, Y., Fukukita, A., Tamura, K., *et al.* (2014),"Seismic response control using electro-magnetic inertial mass damper", *Earthq. Eng. Struct. D.*, **43**(4), 507-527. https://doi.org/10.1002/eqe.2355.

Pacheco, B. M., Fujino, Y. and Sulekh, A. (1993), “Estimation curve for modal damping in stay cables with viscous damper”, *J. Struct. Eng.*, **119**(6), 1961-1979. https://doi.org/10.1061/(ASCE)0733-9445(1993)119:6(1961).

Sun, L.M., Hong, D.X. and Chen, L. (2017), “Cables interconnected with tuned inerter damper for vibration mitigation”, *Eng. Struct.*, **151**, 57-67. https://doi.org/10.1016/j.engstruct.2017.08.009.

Shen, W.A., Zhu, S.Y. and Zhu, H.P. (2016), “Experimental study on using electromagnetic devices on bridge stay cables for simultaneous energy harvesting and vibration damping”, *Smart Mater. Struct.*, **25**(6), 065011.

Shi, X., Zhu S.Y., Li, J.Y., *et al*. (2016), “Dynamic behaviour of stay cables with passive negative stiffness dampers”, *Smart Mater. Struct.*, **25**(7), 075044.

Shi, X., Zhu, S.Y. and Spencer, B.F. (2017), “Experimental study on passive negative stiffness damper for cable vibration mitigation”, *J. Eng. Mech.*, **143**, 04017070. https://doi.org/10.1061/(ASCE)EM.1943-7889.0001289.

Shi, X. and Zhu S.Y. (2018), “Dynamic characteristics of stay cables with inerter dampers”, *J. Sound Vib.*, **423**, 287-305. https://doi.org/10.1016/j.jsv.2018.02.042.

Weber, F. and Distl, H. (2015a), “Amplitude and frequency independent cable damping of Sutong Bridge and Russky Bridge by magnetorheological dampers”, *Struct. Control Health Monit*., **22** (2), 237-254. https://doi.org/10.1002/stc.1671.

Weber, F. and Distl, H. (2015b), “Semi-active damping with negative stiffness for multi-mode cable vibration mitigation: approximate collocated control solution”, *Smart Mater. Struct.*, **24**(11), 115015 (14pp).

Wang, Z.H., Chen, Z.Q., Gao, H., *et al.* (2018), “Development of a self-powered magnetorheological damper system for cable vibration control”, *Appl. Sci.*, **8**(1), 1-17. https://doi.org/10.3390/app8010118.

Wang, Z.H., Gao, H., Fan, B.Q., *et al.* (2018), “Inertial mass damper for vibration control of cable with sag”, *J. Low. Freq. Noise V. A.*, 1-12. https://doi.org/10.1177/1461348418814967

Wang, X.Y., Ni, Y.Q., Ko, J.M, et al. (2005), “Optimal design of viscous dampers for multi-mode vibration control of bridge cables”, *Eng.Struct.*, **27**(5), 792-800. https://doi.org/10.1016/j.engstruct.2004.12.013.

Xu, Y.L. and Yu, Z. (1998), “Vibration of inclined sag cables with oil dampers in cable stayed bridges”, *J. Bridge Eng.*, **3**(4), 194-203. https://doi.org/10.1061/(ASCE)1084-0702(1998)3:4(194).

Xu, Y.L. and Zhou, H.J. (2007), “Damping cable vibration for a cable-stayed bridge using adjustable fluid dampers”, *J. Sound Vib*., **306**(1), 349-360. https://doi.org/10.1016/j.jsv.2007.05.032.

Zhu, H.P., Li, Y.M., Shen, W.A., *et al*. (2019), “Mechanical and energy-harvesting model for electro-magnetic inertial mass dampers”, *Mech. Syst. Signal Pr.*, **120**, 203-220. https://doi.org/10.1016/j.ymssp.2018.10.023.

Zhou, P. and Li, H. (2016), “Modeling and control performance of a negative stiffness damper for suppressing stay cable vibrations”, *Struct. Control Health Monit*., **23**(4), 764-782. https://doi.org/10.1002/stc.1809.

Zhou, H.J. and Sun, L.M. (2008), “Parameter optimization of damper with stiffness for stay cable”, *Chinese Quarterly of Mechanics*, **29**(1), 180-185. (in Chinese)

Zhou, H.J., Sun, L.M. and Xing, F. (2014a), “Damping of full-scale stay cable with viscous damper: experiment and analysis”, *Adv. Struct. Eng.*, **17**(2), 265-274. https://doi.org/10.1260/1369-4332.17.2.265.

Zhou, H.J., Sun, L.M. and Xing, F. (2014b), “Free vibration of taut cable with a damper and a spring”, *Struct. Control Health Monit*., 2014, **21**(6), 996-1014. https://doi.org/10.1002/stc.1628.

Zhou, H.J., Yang, X., Sun, L.M., *et al*. (2015), “Free vibrations of a two-cable network with near-support dampers and a cross-link”, *Struct. Control Health Monit*., **22**(9), 1173-1192. https://doi.org/10.1002/stc.1738.

Zhou, H.J., Qi, S.K., Yao, G.Z., *et al.* (2018a), “Damping and frequency of a model cable attached with a pre-tensioned shape memory alloy wire: experiment and analysis”, *Struct. Control Health Monit*., **25**(2), e2106. https://doi.org/10.1002/stc.2106.

Zhou, H.J., Huang, X.G., Xiang, N., *et al*. (2018b), “Free vibration of a taut cable with a damper and a concentrated mass”, *Struct. Control Health Monit.*, e2251. https://doi.org/10.1002/stc.2251.

Zhou, H.J., Xiang N., Huang, X.G., *et al*. (2018c), “Full-scale test of dampers for stay cable vibration mitigation and improvement measures”, *Struct. Monit. Maint.* **5**(4), 489-506. https://doi.org/10.12989/smm.2018.5.4.489.